Az alacsony dózisteljesítményű, folyamatos sugárzás biológiai hatása: brachiterápia

A sugárbiológia 4 R-je

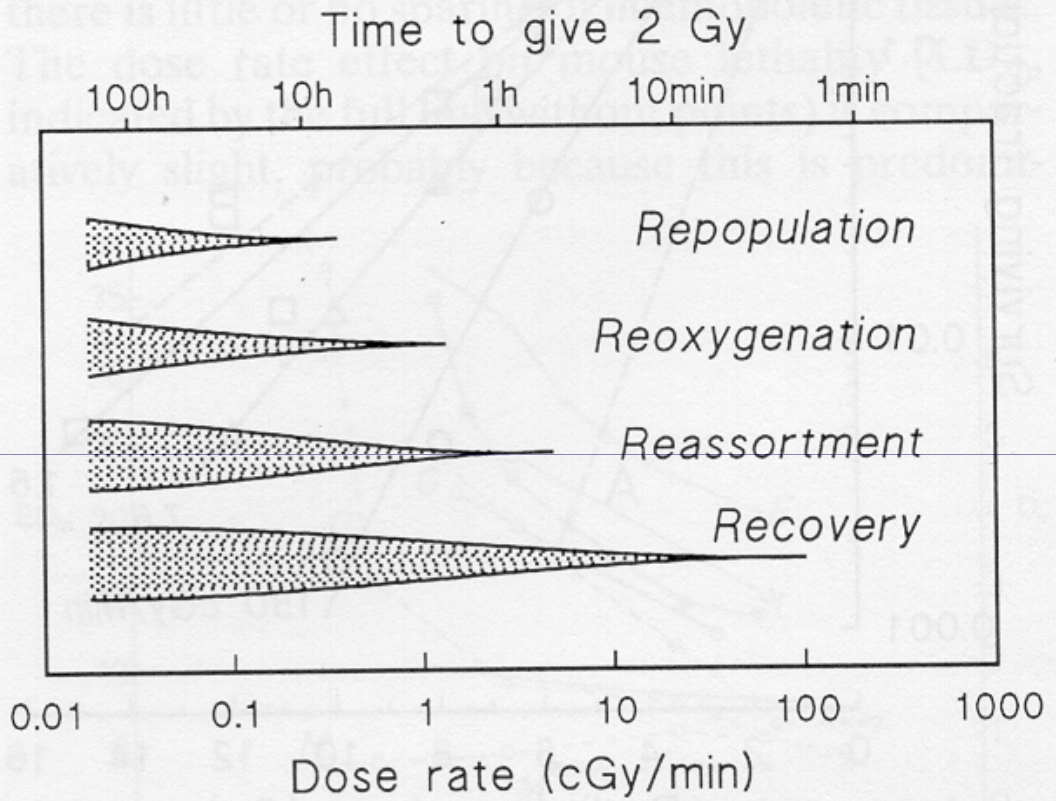

Figure 18.1 The range of dose rates over which repair, reassortment and repopulation modify radiosensitivity depends upon the speed of these processes. From Steel *et al* (1986), with permission.

Az LPL modell

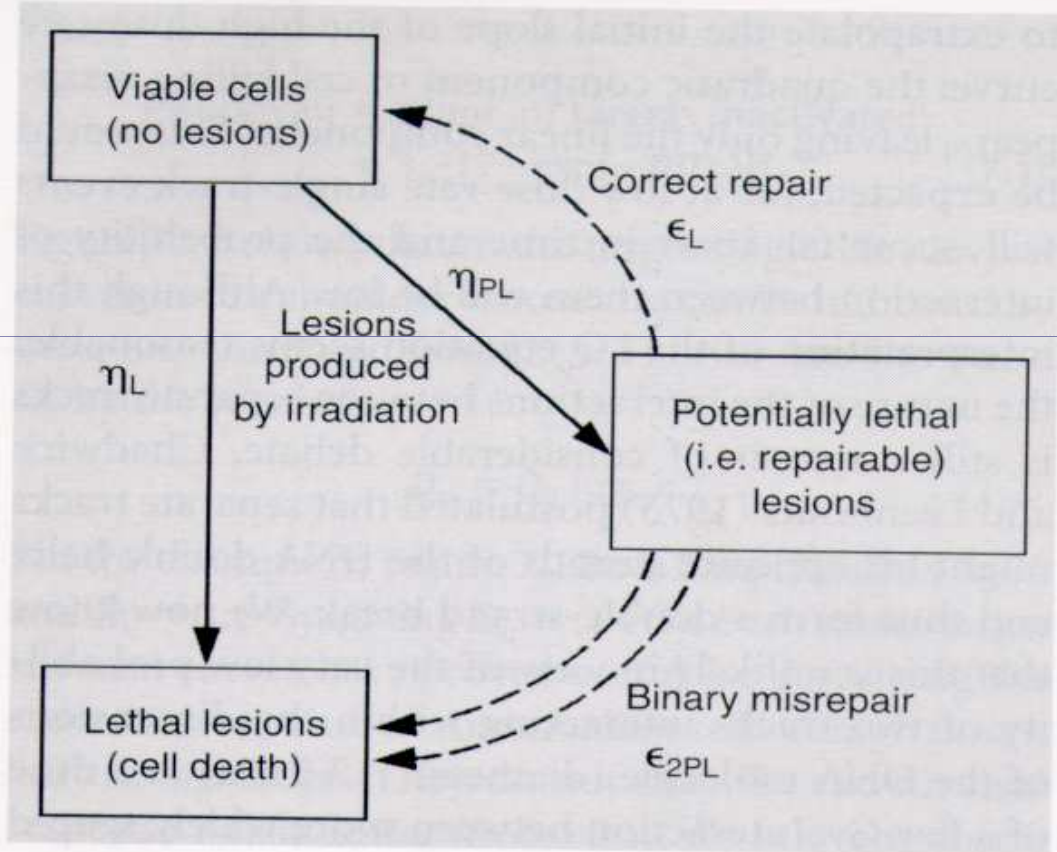

Figure 7.3 *The lethal, potentially lethal (LPL) damage model of radiation action.*

Repair telítési modell

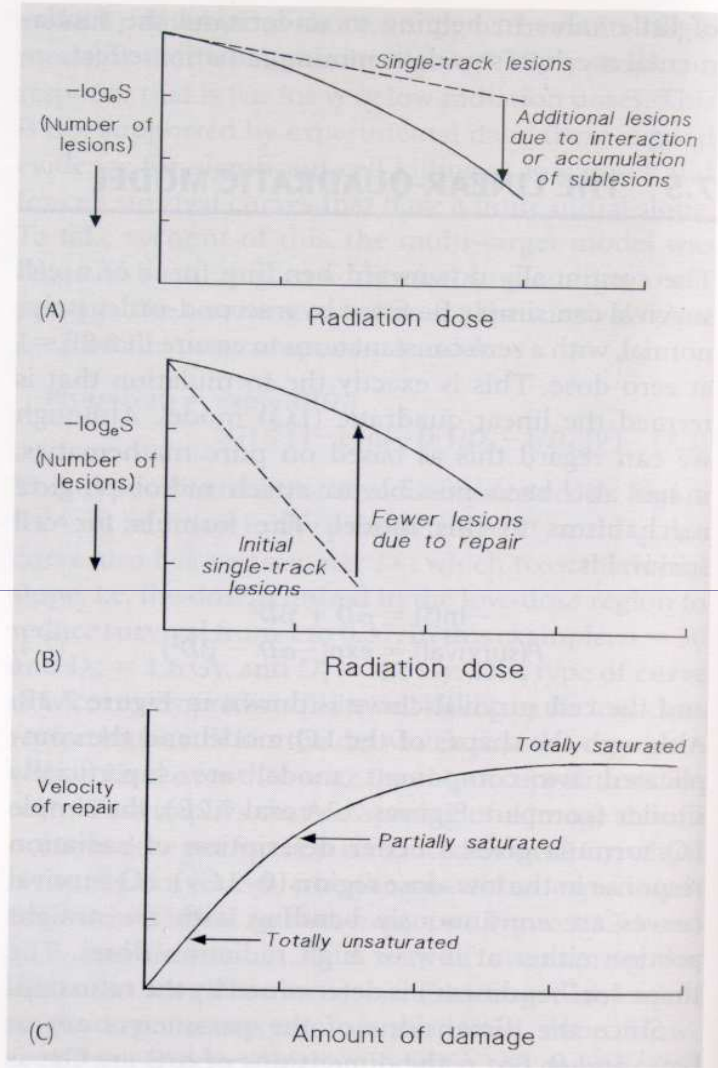

Figure 7.4 *The contrast between lesion-interaction models and repair-saturation models. (A) The LPL model; (B) the effect of repair becoming less effective at higher radiation doses; (C) the basic concept of repair saturation. Adapted from Goodhead (1985), with permission.*

A dózisteljesítmény hatása a sejtek túlélésére

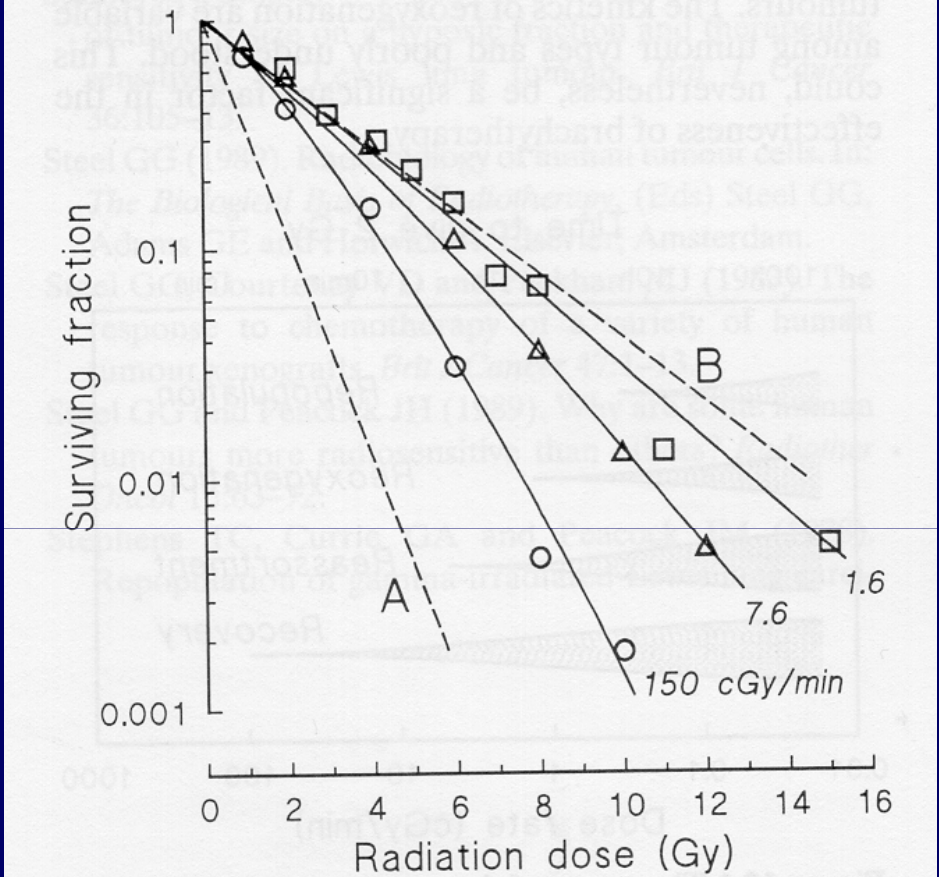

Figure 18.2 Cell survival curves for a human melanoma cell line irradiated at dose rates of 150, 7.6 or 1.6 cGy/min. The data are fitted by the LPL model, from which the lines A and B are derived (see text). From Steel *et al* (1987), with permission.

Dose-recovery factor (DRF)

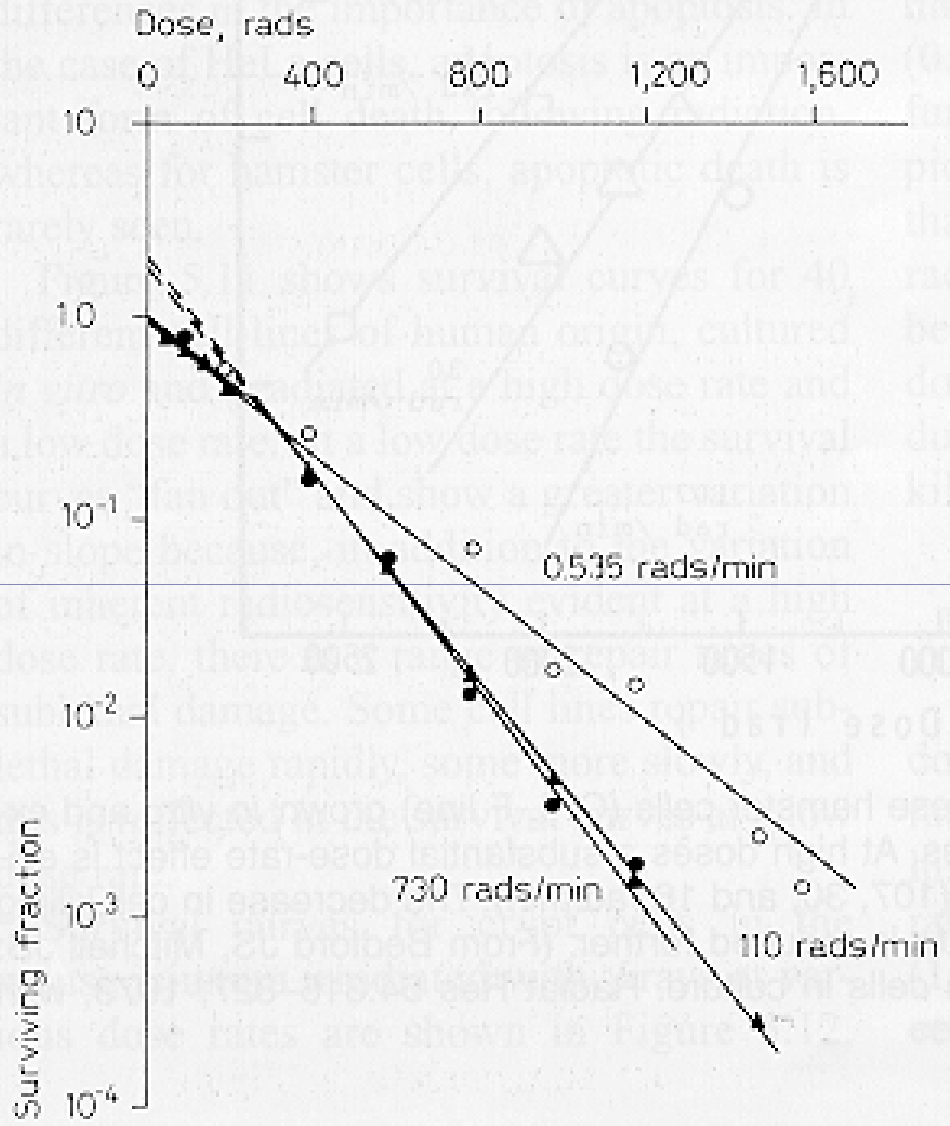

Figure 5.9. Survival curves for HeLa cells exposed to γ-rays at high and low dose rates.

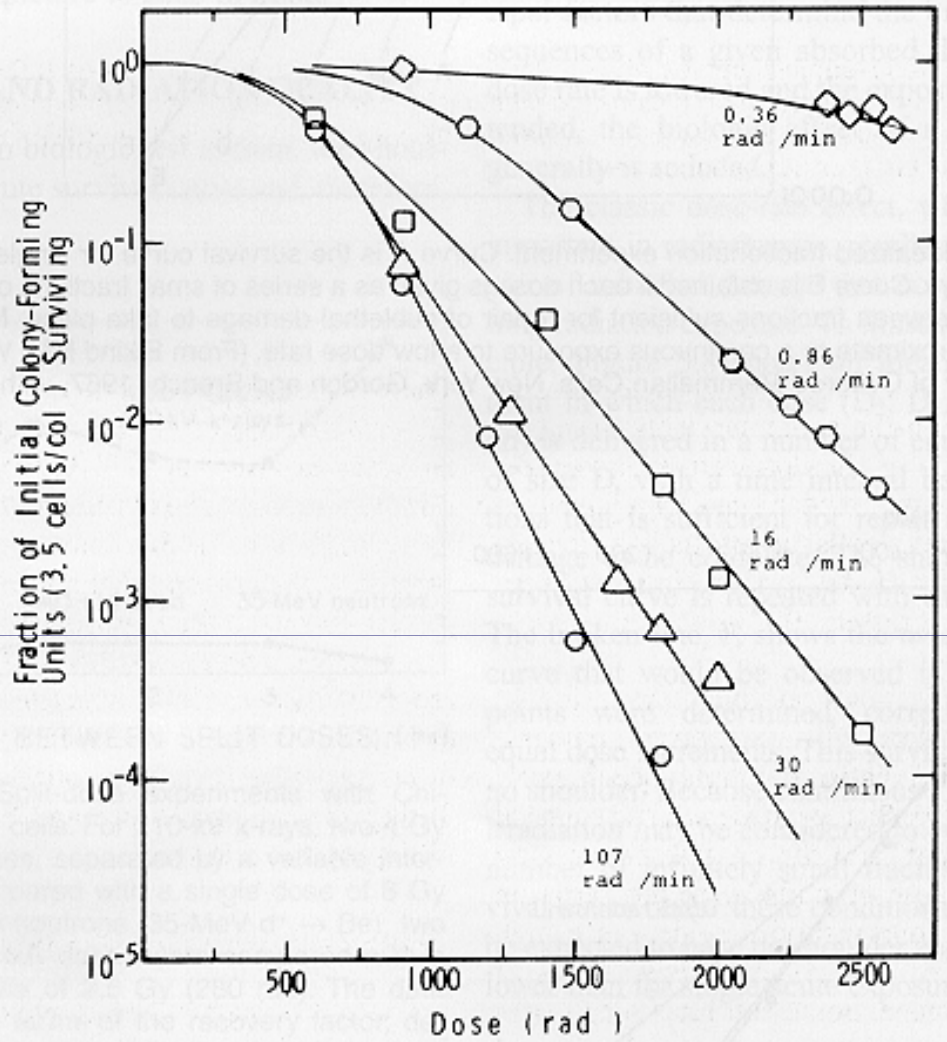

Figure 5.10. Dose–response curves for Chinese hamster cells (CHL-F line) grown *in vitro* and exposed to cobalt-60 γ-rays at various dose rates. At high doses a substantial dose-rate effect is evident even among 1.07, 0.3, and 0.16 Gy/min (107, 30, and 16 rad/min). The decrease in cell killing becomes even more dramatic as the dose rate is reduced further. (From Bedford JS, Mitchell JB: Dose rate effects in synchronous mammalian cells in culture. Radiat Res 54:316–327, 1973, with permission.)

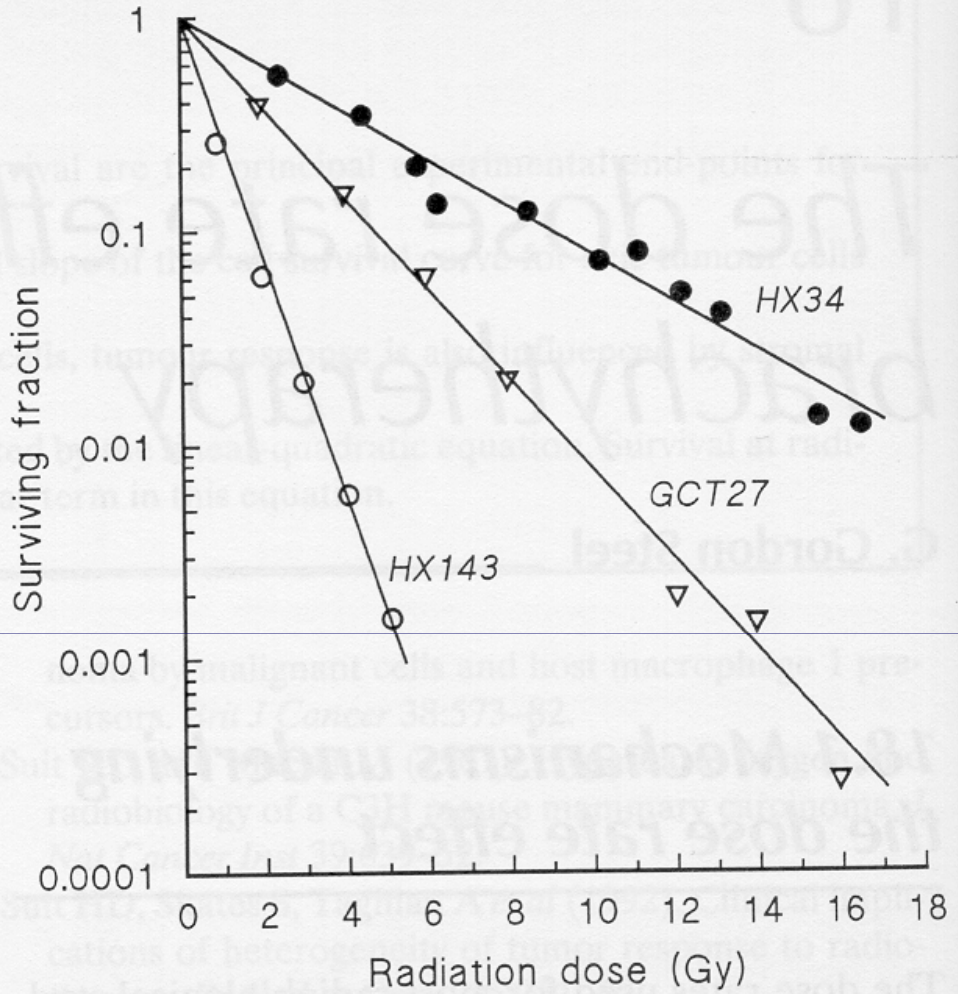

Figure 18.3 Cell survival curves for three human tumour cell lines irradiated at the low dose rate of 1.6 cGy/min. HX143, neuroblastoma; GCT27, germ cell tumour of the testis; HX34, melanoma. From Steel (1991), with permission.

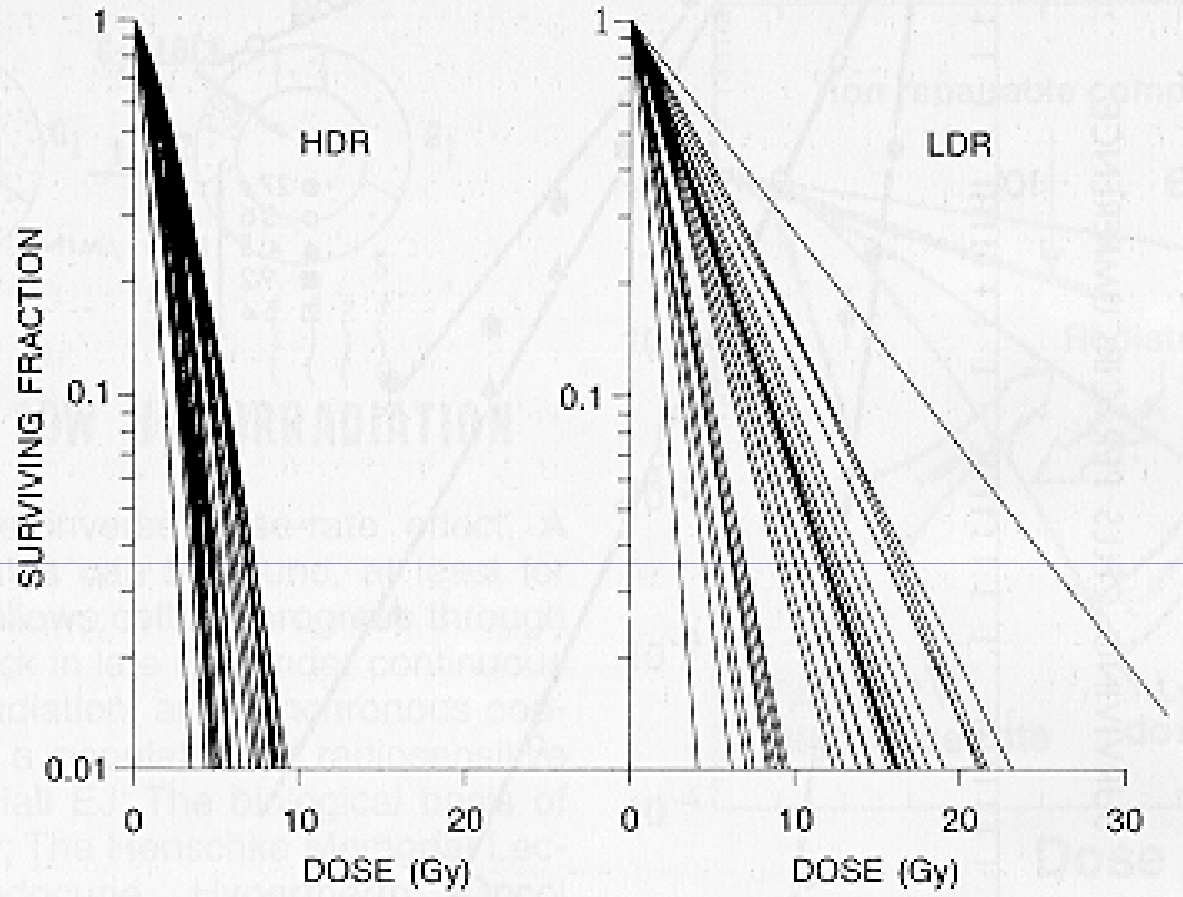

Figure 5.11. Dose–survival curves at high dose rates (HDR) and low dose rates (LDR) for a large number of cells of human origin cultured *in vitro*. Note that the survival curves fan out at low dose rates because in addition to a range of inherent radiosensitivities (evident at HDR) there is also a range of repair times of sublethal damage.

Inverz dózis-teljesítmény

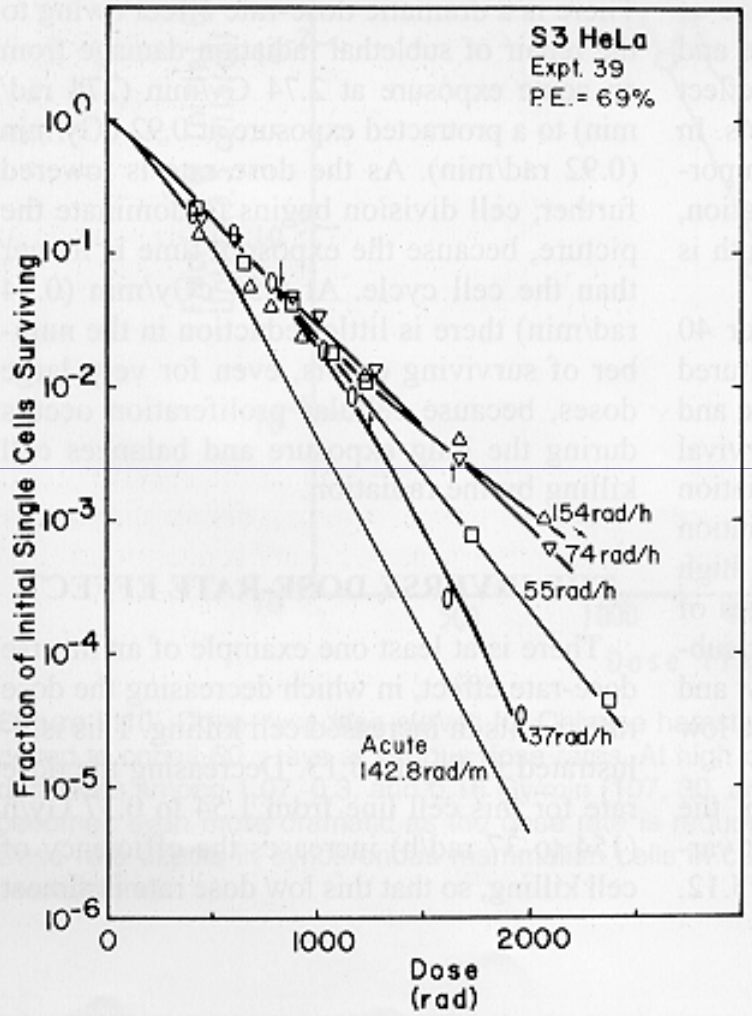

Figure 5.13. The inverse dose-rate effect. A range of dose rates can be found for HeLa cells such that lowering the dose rate leads to more cell killing. At 1.54 Gy/h (154 rad/h), cells are "frozen" in the various phases of the cycle and do not progress. As the dose rate is dropped to 0.37 Gy/h (37 rad/h), cells progress to a block in G_2, a radiosensitive phase of the cycle. (From Mitchell JB, Bedford JS, Bailey SM: Dose-rate effects on the cell cycle and survival of S3 HeLa and V79 cells. Radiat Res 79: 520–536, 1979, with permission.)

A dózisteljesítmény hatása a normál szövetekre

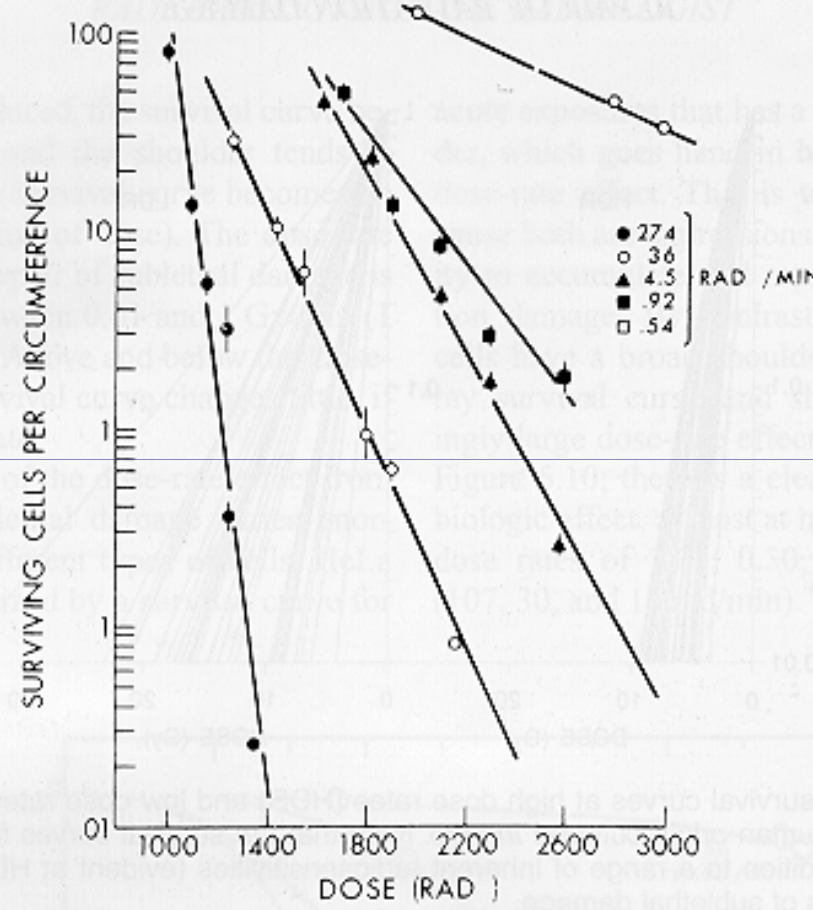

Figure 5.12. Response of mouse jejunal crypt cells irradiated with γ-rays from cesium-137 over a wide range of dose rates. The mice were given total-body irradiation, and the proportion of surviving crypt cells was determined by the appearance of regenerating microcolonies in the crypts 3 days later. Note the large dose-rate effect. (From Fu K, Phillips TL: Radiology 114:709–716, 1975, with permission.)

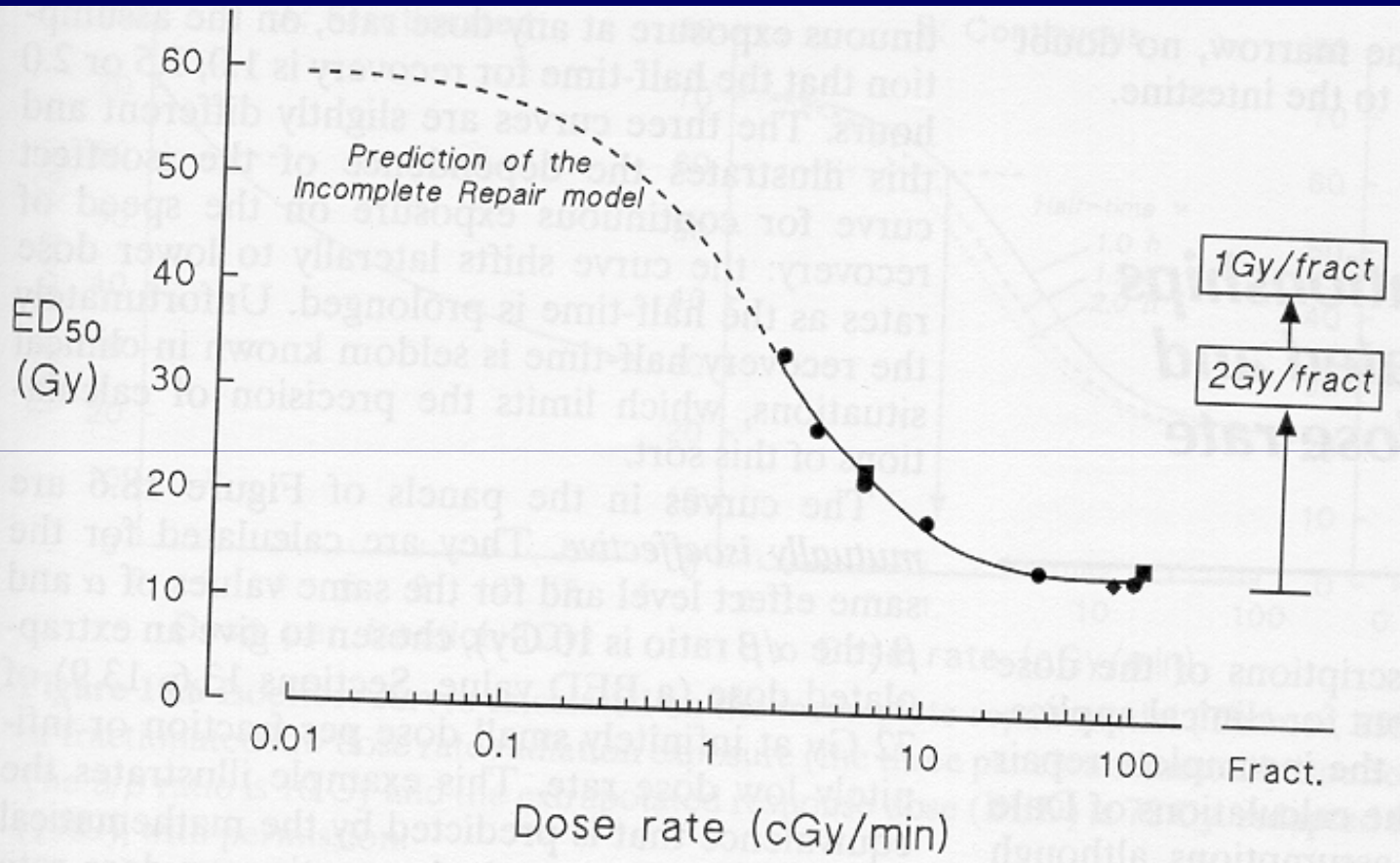

Figure 18.4 The dose rate effect for pneumonitis in mice. The full line fitted to the data was calculated on the basis of the incomplete repair model; the broken line shows its extrapolation to very low dose rates. The boxes on the right show the ED_{50} values for fractionated irradiation. From Down *et al* (1986), with permission.

Alacsony dózisteljesítményű folyamatos besugárzással lehet a terápiát a legrövidebb idő alatt befejezni, a maximális szövet helyreállítás mellett

ED_{50} = 34 Gy = 17 nap x 2 Gy

ED_{50} = 34 Gy = 2 cGy/perc folyamatos = 28 óra

Dózisteljesítmény hatása normál szövetekben

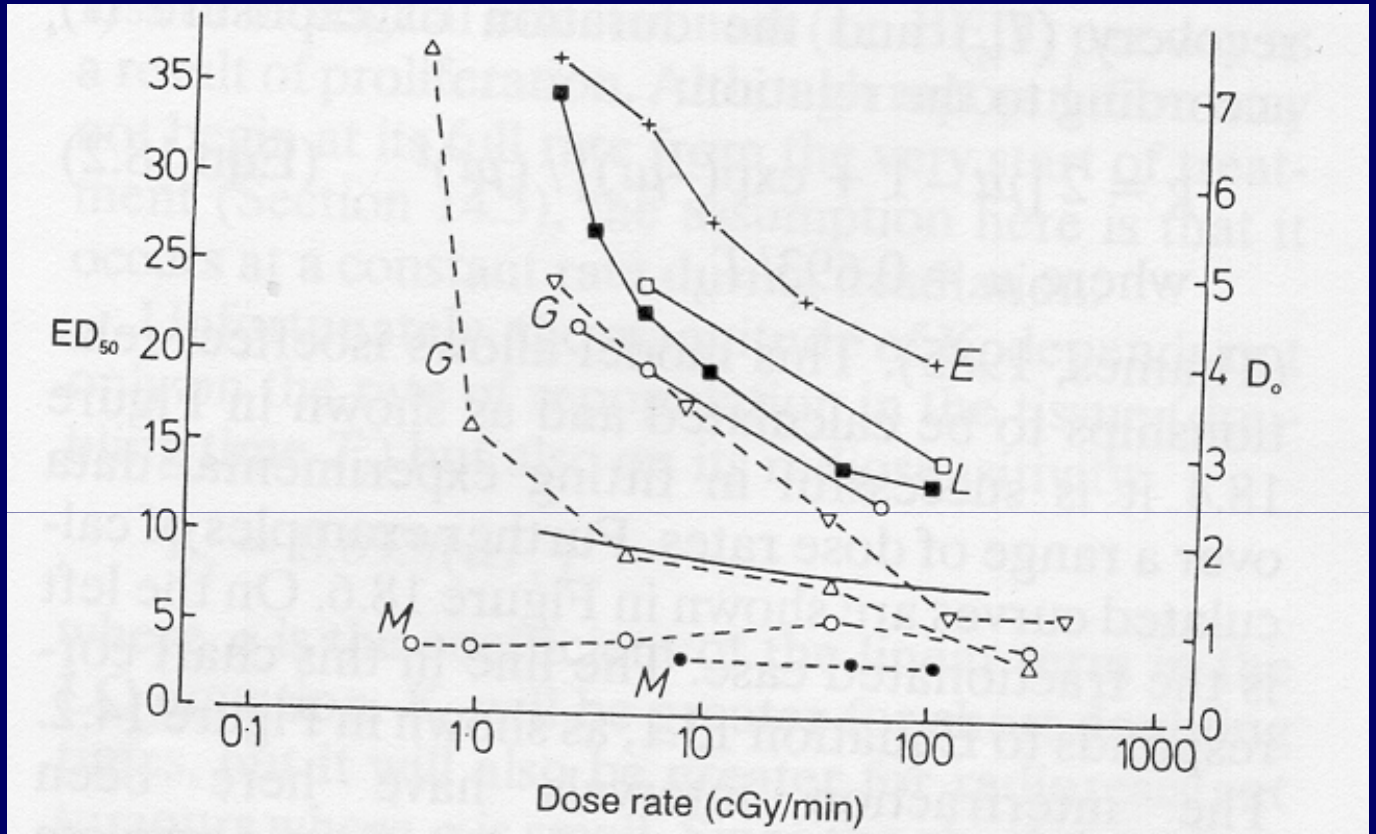

Figure 18.5 The dose rate effect in normal tissues of the mouse: L = lung, G = gut, E = epilation, M = bone marrow. Full lines refer to left-hand scale, dashed lines to right-hand scale. See Steel *et al* (1986) for sources.

Izoeffektus összefüggések a frakcionált és az alacsony dózis-teljesítményű besugárzás között

Inkomplet repair modell

$$E = \alpha D + \beta D^2 g$$

g – idő-függő recovery faktor, függ a repair félidejétől ($T_{1/2}$) és az expozíciós időtől

$$g = 2\,\{\mu t - 1 + \exp(-\mu t)\} / (\mu t)^2$$

$$\mu = 0{,}693 / T_{1/2}$$

Inkomplet repair faktor (g) folyamatos besugárzás esetén

$$BED = D \{1 + Dg/(\alpha/\beta)\}$$

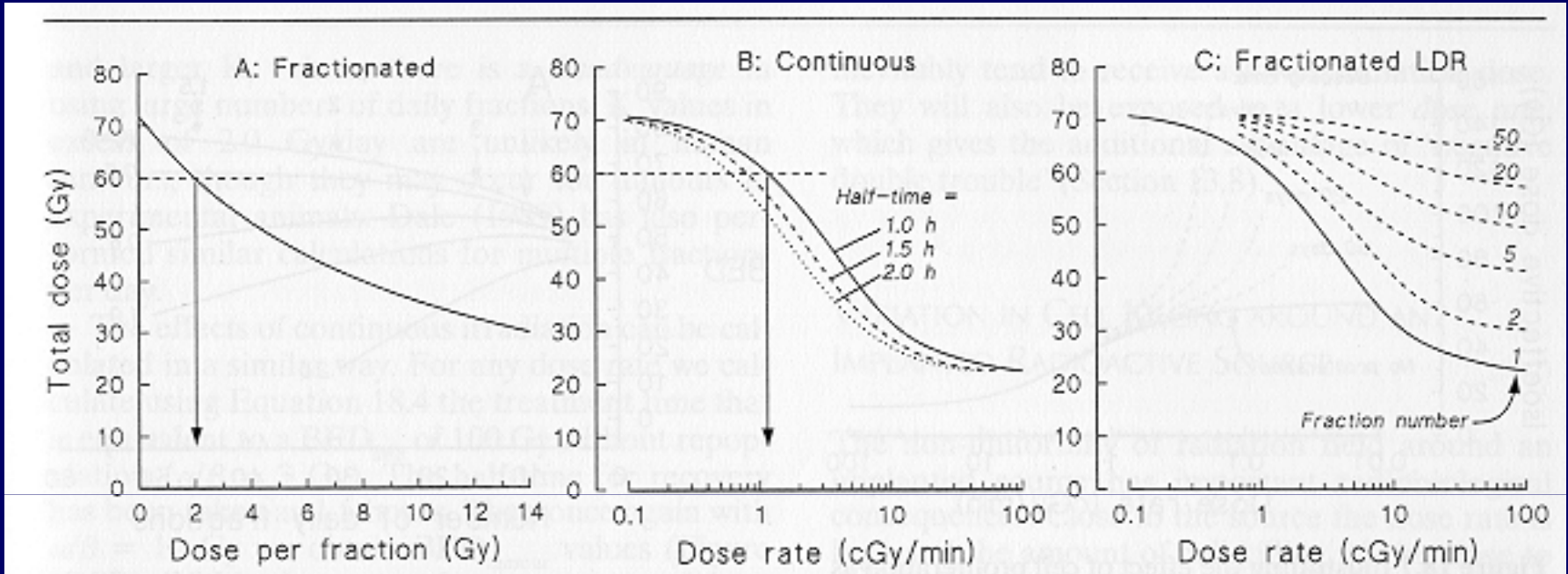

Figure 18.6 Isoeffect curves calculated on the incomplete repair model (Thames, 1985) for fractionated, continuous or fractionated low dose rate radiation exposure (the three panels are mutually isoeffective). Repopulation is ignored. The α/β ratio is 10 Gy and the extrapolated response dose (BED) is 72 Gy. Adapted from Steel (1991) and Steel *et al* (1989), with permission.

30 x 2 Gy = 1 cGy/ perc

6-8 Gy / frakció = 5 cGy / perc

10 Gy 6 frakció = 10 cGy / perc

A sejt-proliferáció hatása

Frakcionált besugárzás

$$BED = D\{1 + d/(\alpha/\beta)\} - K_r T$$

Folyamatos besugárzás

$$BED = D\{1 + gD/(\alpha/\beta)\} - K_r T$$

T – kezelési idő

K_r – a biológiai hatásosság elvesztése (Gy/nap)

$$K_r = 0{,}693/(\alpha T_r)$$

T_r – megkettőződési idő

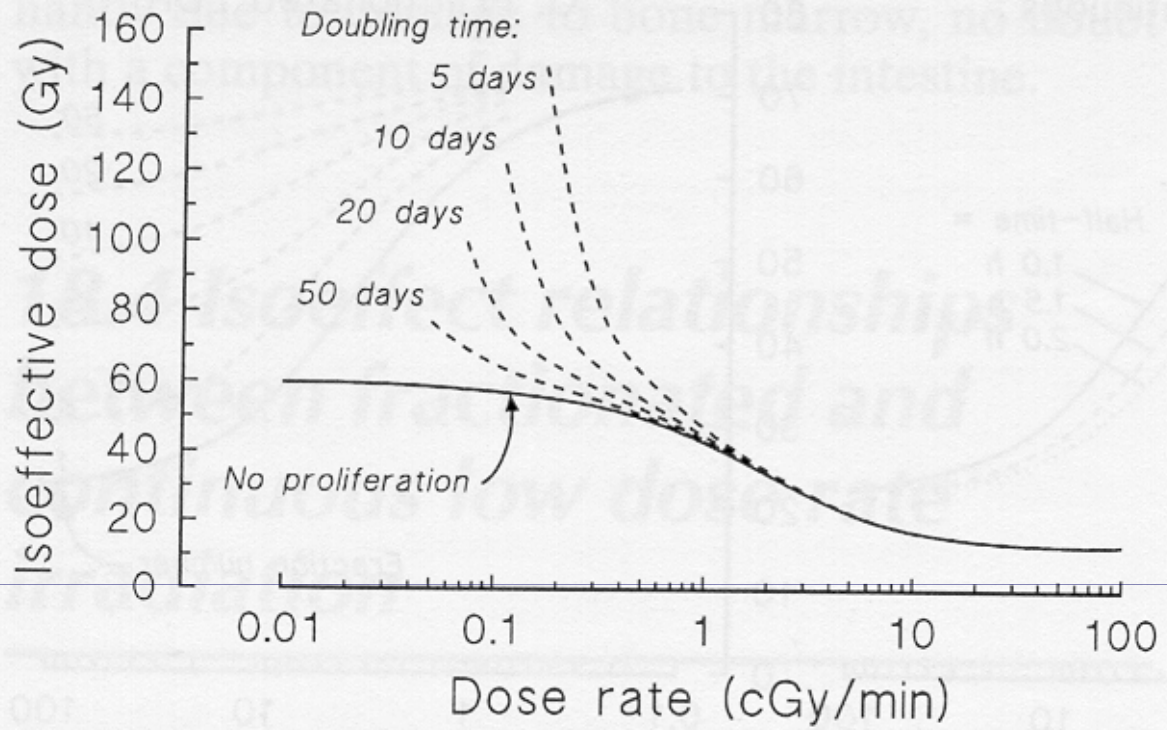

Figure 18.7 Illustrating the effect of cell proliferation as a function of dose rate. Isoeffect curves are shown for no proliferation or with the doubling times indicated. The calculations are based on a simple model of exponential growth, ignoring radiation effects on the rate of cell proliferation.

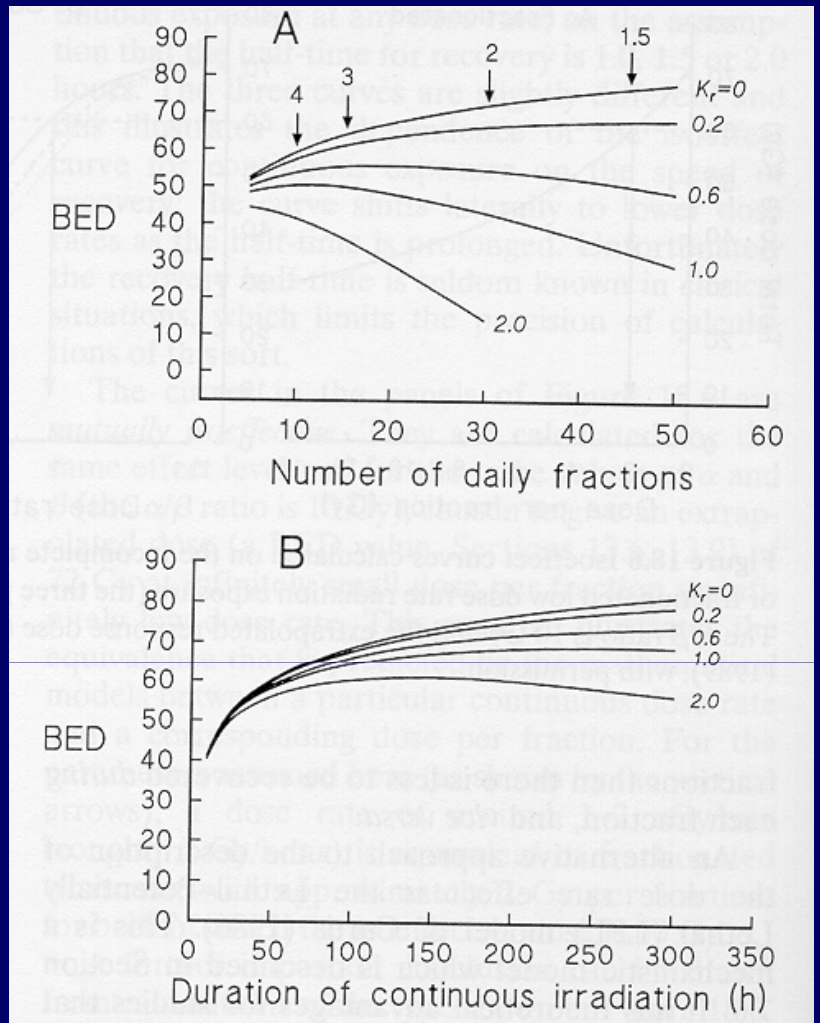

Figure 18.8 Tumour response for a fixed level of late normal-tissue damage as a function of (**A**) fraction number or (**B**) exposure time in a single continuous dose. These curves are recalculated and redrawn after Dale (1989), as described in the text. The arrows in panel **A** indicate the dose per fraction (Gy) at various points along the curve for no tumour cell proliferation ($K_r = 0$).

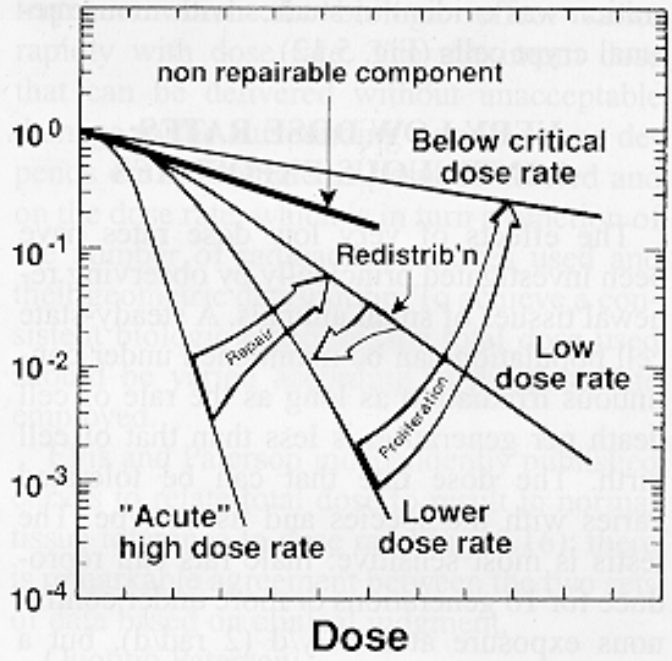

Figure 5.15. The dose-rate effect resulting from repair of sublethal damage, redistribution in the cycle, and cell proliferation. The dose–response curve for acute exposures is characterized by a broad initial shoulder. As the dose rate is reduced, the survival curve becomes progressively shallower as more and more sublethal damage is repaired but cells are "frozen" in their positions in the cycle and do not progress. As the dose rate is lowered further and for a limited range of dose rates, the survival curve steepens again because cells can progress through the cycle to pile up at a block in G_2, a radiosensitive phase, but still cannot divide. A further lowering of dose rate allows cells to escape the G_2 block and divide; cell proliferation then may occur during the protracted exposure, and survival curves become shallower as cell birth from mitosis offsets cell killing from the irradiation. (Based on the ideas of Dr. Joel Bedford.)

Brachiterápia

Rádium
Cézium-137
Iridium-192

Intracavitáris
Intersticiális

TABLE 5.1. *Characteristics of Radionuclides for Intracavitary or Interstitial Brachytherapy*

Radionuclide	Photon Energy, KeV		Half-life	HVL, mm lead
	Average	Range		
Conventional				
Cesium-137	662	—	30 y	5.5
Iridium-192	380	136–1060	74.2 d	2.5
New				
Iodine-125	28	3–35	60.2 d	0.025
Gold-198	412	—	2.7 d	2.5
Americium-241	60	—	432 y	0.125
Palladium-103	21	20–23	17 d	0.008
Samarium-145	41	38–61	340 d	0.06
Ytterbium-169	100	10–308	32 d	0.1

Data computed by Dr. Ravinder Nath, Yale University.

Izoeffektív dózisok a felezési idő figyelembe vételével

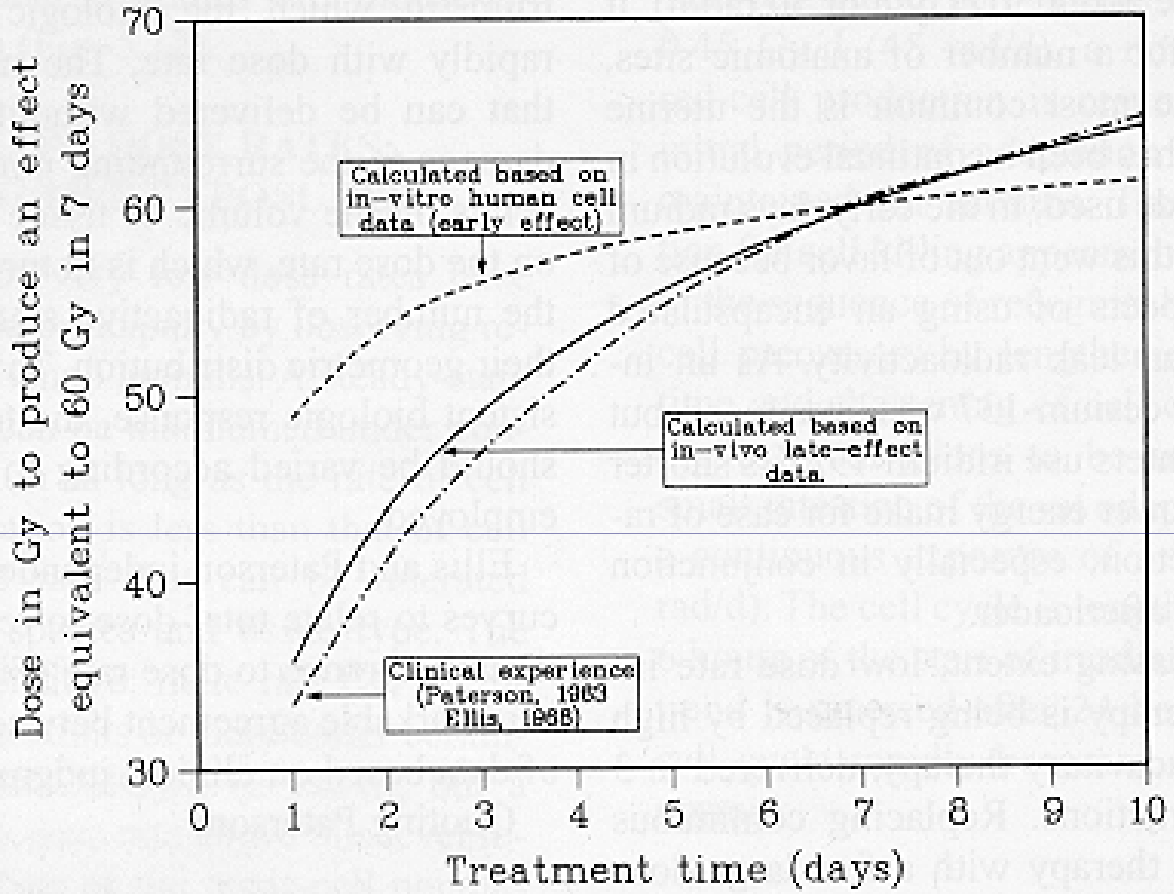

Figure 5.16. Dose equivalent to 60 Gy (6,000 rad) in 7 days as proposed by Paterson (in 1963) and by Ellis (in 1968) based on clinical observation of normal tissue tolerance or calculated from radiobiologic principles. The α/β ratios and the T1/2 for repair of sublethal damage were chosen for early or for late-responding tissues (see Chapter 22).

Dózisteljesítmény hatása a tumor kontrolra és a szövődményekre

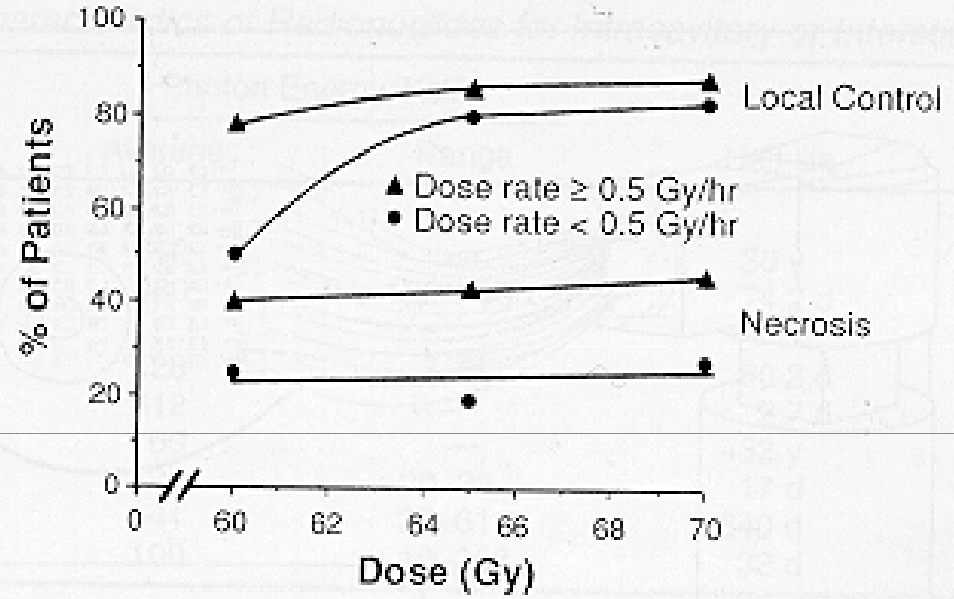

Figure 5.17. Local tumor control and necrosis rate at 5 years as a function of dose in patients treated for T1-2 squamous-cell carcinomas of the mobile tongue and the floor of the mouth with interstitial iridium-192 implants. The patients were grouped according to whether the implant was characterized by a high dose rate (above 0.5 Gy/h or 50 rad/h) or low dose rate (below 0.5 Gy/h or 50 rad/h). The necrosis rate is higher for the higher dose rate at all dose levels. Local tumor control did not depend on dose rate provided the total dose was sufficiently large. (Data from Mazeron JJ, Simon JM, Le Pechoux C, et al: Effect of dose rate on local control and complications in definitive irradiation of T1-2 squamous cell carcinomas of mobile tongue and floor of mouth with interstitial iridium-192. Radiother Oncol 21:39–47, 1991.)

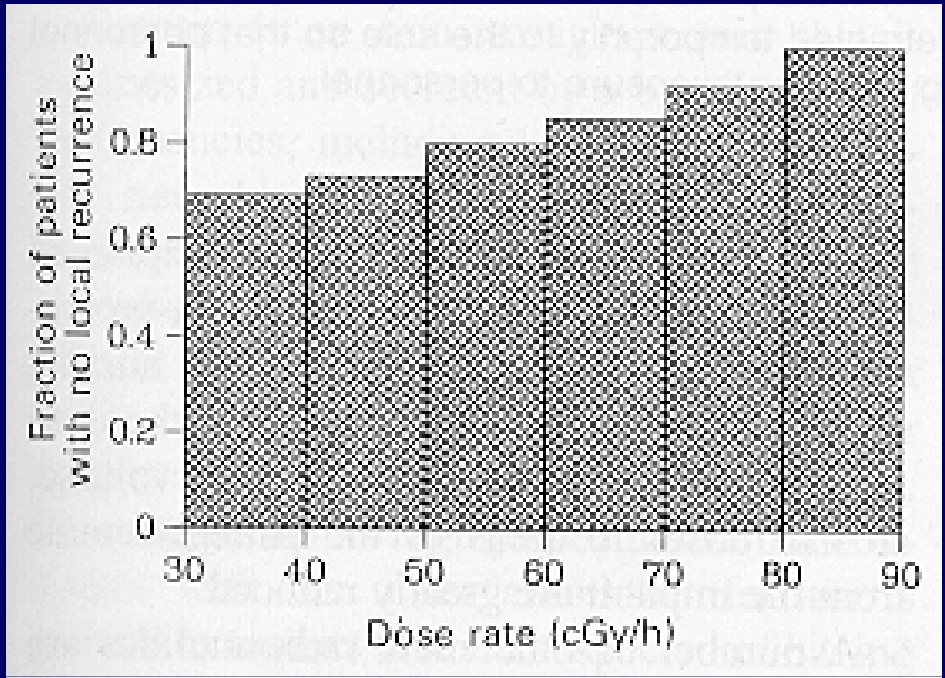

Figure 5.18. Percentage of patients who showed no local recurrence as a function of dose rate in treatment for breast carcinoma by a combination of external-beam irradiation plus iridium-192 interstitial implant. The implant was used to deliver a dose of 37 Gy (3,700 rad); the dose rate varied by a factor of 3, owing to different linear activities of the iridium-192 wire and different volumes implanted. (Data from Mazeron JJ, Simon JM, Crook J, et al: Influence of dose rate on local control of breast carcinoma treated by external beam irradiation plus iridium-192 implant. Int J Radiat Oncol Biol Phys 21: 1173–1177, 1991.)

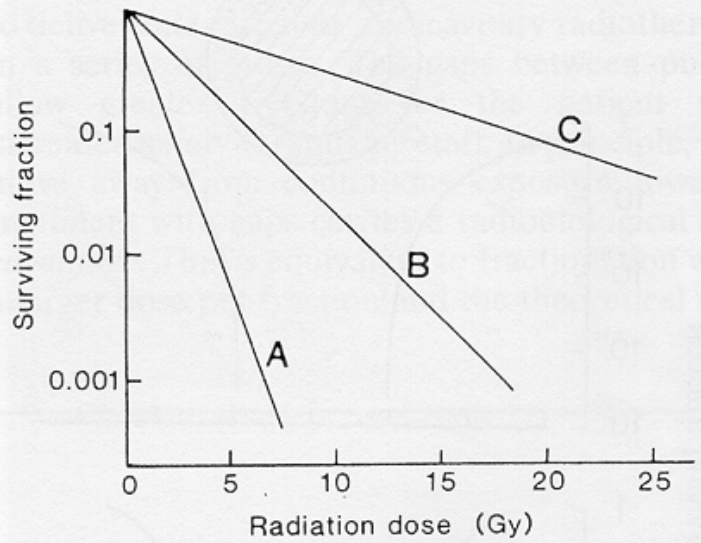

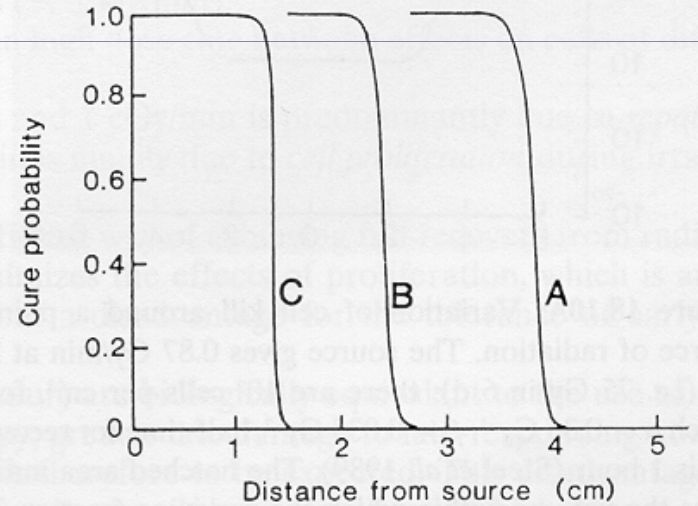

Figure 18.9 The likelihood of cure varies steeply with distance from a point radiation source. The radius at which failure occurs depends upon the steepness of the survival curve at low dose rate. From Steel *et al* (1989), with permission.

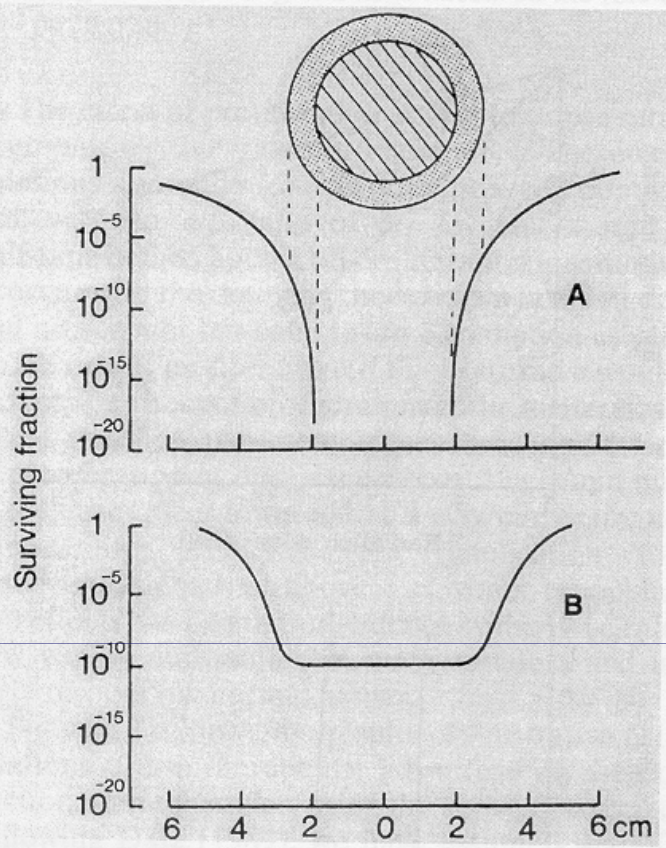

Figure 18.10A: Variation of cell kill around a point source of radiation. The source gives 0.87 Gy/min at 2 cm (*i.e.* 75 Gy in 6 d); there are 10^9 cells per cm^3, for which $\alpha = 0.35\ Gy^{-1}$, $\beta = 0.035\ Gy^{-2}$, half-time for recovery is 1 hour (Steel *et al*, 1989). The hatched area indicates the volume within which the surviving fraction is below 10^{-20}. The stippled area indicates the volume where survival is between 10^{-20} and 10^{-6}, which is the critical region for tumour control. For comparison, panel **B** shows the type of profile that would be aimed for with external-beam radiotherapy.

Alacsony dózis-teljesítményű brachiterápia előnyei

- Normál szövetek kisebb térfogtát éri sugárzás
- A legrövidebb idő alatt lehet a terápiát befejezni

Nagy dózis-teljesítményű pulzáló

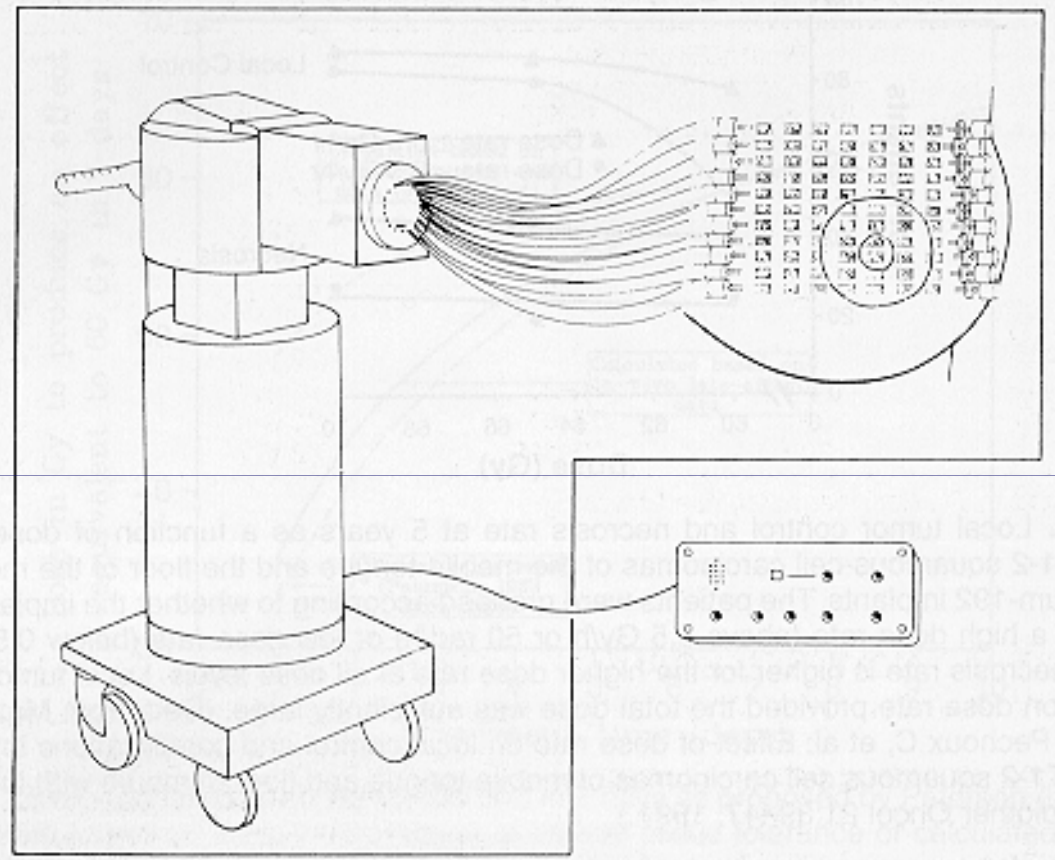

Figure 5.19. Diagram illustrating the use of a computer-controlled remote afterloader to minimize radiation exposure of personnel during brachytherapy. Catheters are implanted into the tumor, and radiographs are made to check the validity of the implant using "dummy" nonradioactive sources. The catheters then are connected to a shielded safe containing the radioactive (iridium-192) sources, which are transferred by remote control to the implant in the patient. The control panel is located outside a lightly shielded room. The sources can be retracted temporarily to the safe so that personnel can care for the patient, thus effectively eliminating radiation exposure to personnel.

Összefoglalás

- Alacsony dózis teljesítményű besugárzás esetén a szubletális károsodások a besugárzás alatt kijavítódnak.
- A kis dózis teljesítményű folyamatos besugárzással a terápia ideje lerövidülhet.

Brachiterápia csökkentheti a besugárzott normál szövetek térfogatát